tvst

https://doi.org/10.1167/tvst.8.4.19

Article

# Retinal Laser Therapy Preserves Photoreceptors in a Rodent Model of MERTK-Related Retinitis Pigmentosa

Seungbum Kang[1], Henri Lorach[2,3], Mohajeet B. Bhuckory[2,3], Yi Quan[3], Roopa Dalal[3], and Daniel Palanker[2,3]

[1] Department of Ophthalmology and Visual Science, College of Medicine, The Catholic University of Korea, Seoul, Republic of Korea
[2] Hansen Experimental Physics Laboratory, Stanford University, CA, USA
[3] Department of Ophthalmology, Stanford University, CA, USA

**Correspondence:** Mohajeet B. Bhuckory, Hansen Experimental Physics Laboratory, 452 Lomita Mall, Stanford University, CA 94305, USA. e-mail: bhuckory@stanford.edu

**Received:** 30 January 2019
**Accepted:** 7 June 2019
**Published:** 7 August 2019

**Keywords:** pattern scanning photocoagulation; selective RPE therapy (SRT); nondamaging retinal laser therapy (NRT); photoreceptors preservation; RCS rat

**Citation:** Kang S, Lorach H, Bhuckory MB, Quan Y, Dalal R, Palanker D. Retinal laser therapy preserves photoreceptors in a rodent model of MERTK-related retinitis pigmentosa. Trans Vis Sci Tech. 2019;8(4):19, https://doi.org/10.1167/tvst.8.4.19


**Purpose:** We investigated the effects of various retinal laser therapies on preservation of the photoreceptors in an animal model of Mer tyrosine kinase receptor (MERTK)–related retinitis pigmentosa (RP). These modalities included photocoagulation with various pattern densities, selective RPE therapy (SRT), and nondamaging retinal therapy (NRT).

**Methods:** Laser treatments were performed on right eyes of RCS rats, using one of three laser modalities. For photocoagulation, six pattern densities (spot spacings of 0.5, 1, 1.5, 3, 4, and 5 spot diameters) were delivered in 19-day-old animals, prior to the onset of photoreceptor degeneration, to determine the optimal treatment density for the best preservation of photoreceptors. The left eye was used as control. Rats were monitored for 6 months after treatment using electroretinography, optical coherence tomography, and histology.

**Results:** Photocoagulation resulted in long-term preservation of photoreceptors, manifested morphologically and functionally, with the extent of the benefit dependent on the laser pattern density. Eyes treated with a 1.5 spot size spacing showed the best morphologic and functional preservation during the 6-month follow-up. SRT-treated eyes exhibited short-term morphologic preservation, but no functional benefit. NRT-treated eyes did not show any observable preservation benefit from the treatment.

**Conclusions:** In a rodent model of MERTK-related RP, pattern photocoagulation of about 15% of the photoreceptors (1.5 spot diameter spacing) provides long-term preservation of photoreceptors in the treatment area.

**Translational Relevance:** Availability of retinal lasers in ophthalmic practice enables rapid translation of our study to clinical testing and may help preserve the sight in patients with photoreceptor degeneration.

## Introduction

Retinitis pigmentosa (RP) is a group of inherited retinal degenerations characterized by progressive loss of photoreceptors, with a prevalence of approximately 1 in 4000.[1] The persistent loss of rod photoreceptors leads to night blindness, followed by loss of cone photoreceptors, which is associated with constriction of the visual field in the daytime, deterioration of visual acuity, and eventually blindness after several decades.[2] Novel treatments for slowing the disease progression or restoring sight have been investigated, including gene therapy,[3,4] stem cell transplantation,[5,6] neuroprotection,[7] and retinal prosthesis.[8]

To date, numerous genetic mutations have been identified as the cause of RP, which explains the heterogeneity of the disease and the difficulty in finding a universal treatment.[9] However, a particular form of RP resulting from mutations of the Mer tyrosine kinase receptor (MERTK) gene may be closer to potential treatment. Such mutations account for approximately 1% to 2.5% of RP cases.[10,11]

MERTK is responsible for the efficient phagocytosis of shed photoreceptor outer segments (POS) by the retinal pigment epithelium (RPE).[12] Therefore, mutations in this gene impair phagocytosis and lead to accumulation of shed POS and subsequent formation of subretinal debris. Eventually, this mutation causes gradual loss of photoreceptors.[13]

Long-term functional and morphologic preservation of photoreceptors has been demonstrated after viral vector gene replacement therapy in Royal College of Surgeons (RCS) rats, an RP animal model of the MERTK gene mutation.[14–16] However, long before the development of MERTK gene therapies, studies have reported rescue of photoreceptors in this animal model following laser photocoagulation.[17–19] While the mechanism leading to the rescue effect remained unknown, some studies have suggested that the laser treatment somehow enhanced phagocytosis or increased β-fibroblast growth factor level, promoting the photoreceptor survival.

In a previous study, we showed that laser photocoagulation in RCS rats results in long-term preservation of photoreceptors.[20] We hypothesized that although mutations in the MERTK gene impair phagocytosis, minimal phagocytic activity of RPE cells still remained, possibly via MERKT-independent mechanisms. Therefore, eliminating a fraction of photoreceptor cells would result in less daily shedding of POS. The RPE cells with reduced phagocytic ability could then sustain the lower POS recycling load to prevent their accumulation, thus delaying the photoreceptor degeneration. Our previous study showed that 1.5-spot diameter (d) spacing laser photocoagulation were morphologically and functionally preserved to photoreceptors for nearly three times longer compared to untreated eyes. However, prior to clinical trial of this treatment, it is essential to investigate the optimal dosimetry: the fraction of photoreceptors to be eliminated for the best preservation of the visual function. If too many photoreceptors are eliminated, the amount of daily POS shedding would be smaller, but the overall retinal function would be compromised. In contrast, if not enough photoreceptor cells are eliminated, the subretinal POS accumulation rate would still be disproportionally higher than the RPE phagocytic rate, leading to formation of a thick debris layer interfering with the oxygen and nutrient flow from the choroid. Therefore, there should be an optimal laser treatment density that causes minimal acute damage but maximizes long-term preservation of the photoreceptors. We used a computer-guided pattern scanning laser (PASCAL) to determine the optimal fraction of photoreceptors to be eliminated by adjusting the laser pattern density.

Selective RPE therapy (SRT) and nondamaging retinal therapy (NRT) have also been used in clinics to treat common retinal disorders such as central serous chorioretinopathy,[21] diabetic macular edema,[22,23] and macular telangiectasia.[24] SRT selectively eliminates RPE cells via explosive vaporization of melanosomes without damaging the photoreceptor cells.[25,26] Following treatment, RPE cells from adjacent areas migrate and proliferate, effectively refilling the damaged area. One week after SRT, the ablated zone in the RPE layer was completely refilled, including many small proliferating RPE cells, which, importantly, outnumber the original RPE cells.[27] Thus, when applied to RCS rats, the number of RPE cells available to handle POS shedding could increase, thereby delaying photoreceptor degeneration.

NRT, the nondamaging retinal laser therapy based on the Endpoint Management (EpM) titration protocol,[24,28] induces thermal stress of RPE cells below the damage threshold.[29] Although the exact mechanism leading to therapeutic benefits of NRT is not clear, it is thought that sublethal thermal stress results in upregulation of a heat-shock proteins. These proteins boost recycling of accumulated misfolded proteins, thereby rejuvenating RPE cells and restoring their cellular function.[24] Thus, RPE cells stimulated by NRT might be able to recycle the shed outer segments more effectively.

In this study, we investigated the optimal laser pattern density of photocoagulation, as well as the effects of SRT and NRT, on preservation of photoreceptors in an animal model of MERTK-related RP.

## Materials and Methods

### Animals

Pigmented RCS rats were obtained from the Rat Resource and Research Center (RCS-p+/LavRrrc strain; University of Missouri, Columbia, MO) and housed under 12/12-hour light-dark illumination. A total of 46 RCS rats were used in accordance with the Association for Research in Vision and Ophthalmology Statement for the Use of Animals in Ophthalmic and Vision Research. All proposed experiments were reviewed and approved in advance by the Administrative Panel on Laboratory Animal Care at Stanford

University. Postnatal 19-day-old (P19) RCS rats were randomly divided into three groups according to laser treatment modality: photocoagulation ($n = 30$), SRT ($n = 8$), and NRT ($n = 8$). Prior to laser treatment, electroretinogram (ERG) recordings, or optical coherence tomography (OCT) imaging, animals were anesthetized with ketamine hydrochloride (75 mg/kg) and xylazine (5 mg/kg) delivered by intramuscular injection, and their pupils were dilated using one drop of 1% tropicamide and 2.5% phenylephrine hydrochloride. Topical 0.5% tetracaine hydrochloride was instilled in the eye for local anesthesia.

## Laser Treatments

For photocoagulation, a total of 30 RCS rats were divided into six subgroups ($n = 5$ per subgroup). A 577-nm PASCAL laser (Topcon Medical Laser Systems, Santa Clara, CA) was used to deliver uniformly patterned laser lesions. Before photocoagulation, preliminary test spots were applied to P19 RCS rats to determine the appropriate pulse energy level for creating barely visible retinal coagulation lesions. The laser parameters were as follows: typical power of 40 mW, duration of 15 milliseconds, and aerial spot diameter of 100 µm (45 µm on the rat retina). Using a square grid pattern, six laser pattern densities (spot spacing of 0.5, 1, 1.5, 3, 4, and 5 d) were applied to each subgroup. Irradiation was applied to the central retina, with an irradiated area of approximately 4 $mm^2$ (2 mm $\times$ 2 mm) for each subgroup. The right eye was laser treated, and the fellow left eye served as a control.

For SRT, eight rats were treated with a 532-nm PASCAL laser using a continuous line scanning mode. With a scanning speed of 6.6 m/s (in air), exposure time, defined by the ratio of the beam diameter (100 µm in air) to the beam velocity, is 15 microseconds. Lines of 2 mm in length have been applied 200 µm apart using laser power of 1.5 W, and this was repeated twice in the same location with a 20-millisecond delay. After SRT, fluorescence angiography (FA), OCT, and autofluorescence (AF) imaging were performed to confirm selective RPE damage. If photoreceptor damage was detected on OCT, such eye was excluded from the follow-up. The total treatment area was approximately 6 $mm^2$ (2 mm $\times$ 3 mm).

For NRT, the 577-nm PASCAL laser with EpM was used. First, to determine the laser power for barely visible retinal coagulation lesions, preliminary test spots were applied to the retina of P19 RCS rats with a 15-millisecond duration and a 200-µm spot size. The pulse energy for a barely visible lesion was assigned a 100% EpM setting. A total of eight P19 rats were treated with a pattern-scanned (5 $\times$ 5) grid with 0.25-d spacing, using 30% of the titration energy level (30% EpM setting).[24] The typical laser power on titration was 60 mW. A total of eight (5 $\times$ 5) grid patterns were applied to each animal to ensure coverage of approximately 4 $mm^2$ (2 $\times$ 2 mm). The right eye was laser treated, and the left eye served as a control. After laser treatment, FA, OCT, and AF imaging were performed to check for any signs of retinal damage. If any damage was detected, the eye was excluded from the follow-up.

## Full-Field and Multifocal ERGs

For full-field ERGs, animals were prepared under a dim red light (<1 lux) after overnight dark adaptation. Under anesthesia, pupils were dilated using 1% tropicamide and 2.5% phenylephrine eyedrops, and corneas were lubricated with 1% methylcellulose. A reference/ground needle electrode was placed subcutaneously on the nose. ERG response was recorded from both eyes simultaneously, using an electroretinograph (Espion E2; Diagnosys LLC, Lowell, MA). For dark-adapted full-field ERG responses, stimuli were presented at six increasing intensities of 0.0001, 0.001, 0.01, 0.1, 1, and 3 cd·s/$m^2$. ERG recordings consisted of 10 presentations of a single 1-millisecond flash with a constant 10-second interstimulus interval to verify reproducibility and to improve the signal-to-noise ratio by averaging. Full-field ERGs were recorded at P38, P52, P73, P98, P120, P150, and P180.

For multifocal ERGs, a recording electrode was placed at the corneal limbus. Subcutaneous nose needle electrodes served as a reference and ground electrodes. Before multifocal ERG recordings, the eye was aligned with the center of a monitor (model P2017H; Dell, Round Rock, TX) and placed 11 cm away from it. Multifocal ERG recordings were obtained from each eye. A pseudorandom binary sequence of black and white squares was generated for the stimulus pattern using software (MATLAB and Statistics Toolbox, Release 2015b; MathWorks, Natick, MA), in which the luminance of the squares was either 250 cd/$m^2$ (light) or 0.25 cd/$m^2$ (dark); each frame was presented for 100 milliseconds, followed by a black screen for 400 milliseconds (2-Hz image switch). The multifocal ERG signals were analyzed offline using a custom MATLAB script.

### OCT Imaging

Spectral-domain OCT images were obtained at P19, P38, P52, P73, P98, P120, P150, and P180 by using a diagnostic imaging platform (HRA2-Spectralis; Heidelberg Engineering, Heidelberg, Germany). Before imaging, pupils were dilated, and 1% methylcellulose was used throughout the procedure. During imaging, the cornea was covered with viscoelastic gel and a coverslip to cancel its optical power. Multiple horizontal linear scans were obtained from the optic disc toward the superior retina; a single vertical line was also obtained. Outer nuclear layer (ONL) thickness was measured at five points along the same horizontal line, approximately two disc diameters superior to the optic disc. ONL thicknesses measured in the laser-treated and control eyes were averaged and plotted as a function of age for all animals.

### Histology

All animals in the study were killed at the end of the follow-up (P180) for histologic analysis. Before enucleation, the superior edge of the eye was marked with one stitch under deep anesthesia. Both eyes of each animal were enucleated and fixed in 1% paraformaldehyde and 1.25% glutaraldehyde fixative prepared with 5 mM calcium chloride and 5% sucrose for 24 hours at room temperature. After removal of the cornea and lens, the posterior eye cup was dehydrated through a graded series of alcohols, infiltrated in propylene oxide, and embedded in epoxy. Sections 0.5 μm in thickness were taken using an ultramicrotome (Reichert Ultracut E; Leica, Deerfield, IL) and stained with 0.5% toluidine blue. Serial sections of the slides were photographed by a light microscope (Eclipse E1000; Nikon, Tokyo, Japan). Two images (20×) taken at a similar area from each sample, in the superior and inferior retina of each eye, were used to count photoreceptor nuclei in 100-μm length of the retina.

### Data Analysis

Statistical analyses were performed using statistical software (R, version 3.4.2, Foundation for Statistical Computing, Vienna, Austria). Statistical significance of the differences in b-wave amplitude, ONL thickness, and number of nuclei in the ONL between the laser-treated and control eyes were determined using a paired *t*-test. A $P$ value $< 0.05$ was considered statistically significant.

## Results

### Laser Treatments

Photocoagulation using six laser pattern densities was applied to the retina of the right eye in each group. FA shows hyperreflective spots where the laser treatment was applied, indicating disruption of the RPE (Fig. 1A; 1.5- and 5-d spacing shown). Photoreceptor damage caused by the laser was clearly visible on OCT (Fig. 1A, arrows). The SRT-treated area can be seen as multiple hyperfluorescent lines on FA and as hyporeflective lines on AF images, indicating the destruction of RPE cells. However, OCT shows no detectable damage to photoreceptors (Fig. 1B). Following NRT, no detectable damage of the photoreceptors or RPE layer was identified in FA, AF, or OCT (Fig. 1C).

### ERGs Following Laser Photocoagulation

Figure 2A shows a series of ERG waveforms from RCS rats treated with a laser pattern spacing of 1.5 d. Waveforms in the treated eye decline slower with time than in the control eye. Other representative ERG waveforms from other laser pattern densities are shown in Supplementary Figure S1. Comparison of the b-wave amplitude between the treated and control eyes for various pattern densities over time is shown in Figure 2B. The sparsest laser pattern of 5-d spacing did not provide any benefit compared to a control eye. With a spacing of 4 d, there was a slight improvement in b-wave amplitude, statistically significant ($P < 0.05$) only at day 98. Pattern densities of 1.5- and 3-d spacings exhibited the most significant improvement in ERG response. In the 3-d spacing group, the benefit was sustained up to P120, while with 1.5-d spacing, it lasted until P150. However, with much denser pattern, 0.5-d spacing, ERG decreased right after the laser treatment due to destruction of a very significant fraction of photoreceptors, and even though its decline was slowed down, compared to control, significant benefit was observed only at P73 and P98. Therefore, the laser pattern density of 1.5 d was optimal for functional preservation.

### OCT Following Laser Photocoagulation

At P19, when photocoagulation was applied, retinal structure appears nearly normal on OCT, with all its layers, including the inner nuclear layer (INL) and ONL, photoreceptor inner/outer segments, and RPE clearly visible (Fig. 3A). At P38, the outer

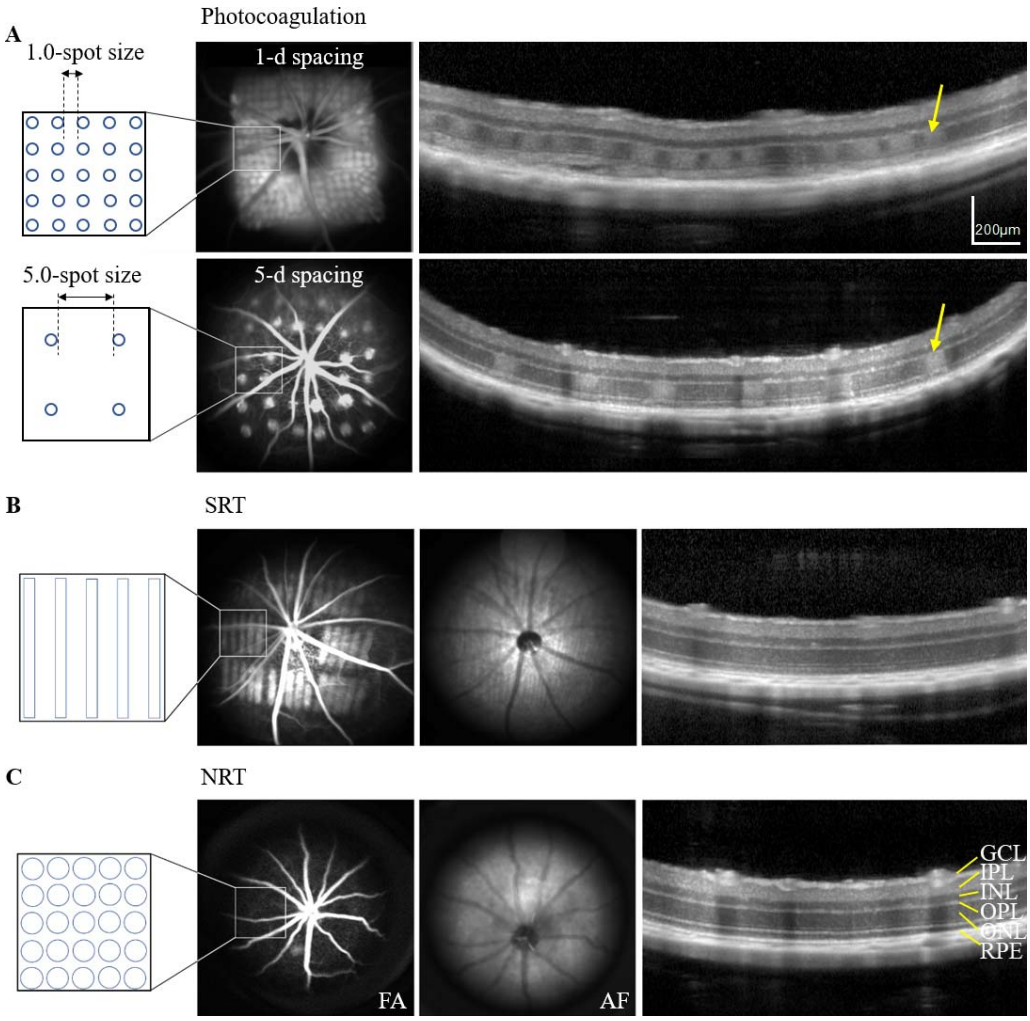


**Figure 1.** Representative images of three different laser treatments of the retina in P19 RCS rats: photocoagulation, SRT, and NRT. Photocoagulation was performed using one of six laser pattern densities (0.5-, 1-, 1.5-, 3-, 4-, and 5-d). (A) FA and a diagram show laser spots applied onto the retina, separated by a distance equivalent to 1 d (*top*) or 5 d (*bottom*). Photoreceptor damage after laser photocoagulation can be seen on OCT (*arrows*). (B) SRT with 15-microsecond exposures using continuous line scanning laser. Selective RPE cell damage is confirmed by multiple hyperfluorescent lines on the FA and hypoautofluorescent lines on the AF image. No photoreceptor damage can be seen on OCT. (C) NRT was delivered using EpM algorithm (30% setting). Neither photoreceptor nor RPE cell damage can be seen on FA, AF image, or OCT.

segments of photoreceptors began to accumulate and form subretinal debris, visible as a thick hyperreflective layer, followed by a progressive thinning of ONL and INL. In control eyes, ONL was not distinguishable after P98 (Fig. 3A). In laser-treated eyes, however, ONL preservation was clearly observed until the end of the follow-up period (P180; Fig. 3A, arrow, 1.5-d spacing). OCT images from other laser pattern densities are shown in Supplementary Figure S2.

Thicker ONL was observed in laser-treated eyes for all pattern densities (Fig. 3B). Longevity of the benefit increased with increasing pattern density: from P73 at 5-d patterns, to P98 at 4- and 3-d spacing, to P180 with denser patterns. However, in the densest pattern (0.5-d spacing), the ONL thickness decreased below that of control eyes after the laser treatment (at P38), indicating excessive laser-induced retinal damage. Again, pattern of 1.5-d spacing provided the best preservation in terms of the ONL thickness.

## Retinal Preservation Localized to the Laser Treatment Zone

Multifocal ERG demonstrated retinal responses only in the laser-irradiated areas and not in untreated retina of right eyes, nor in controls (Fig. 4A). OCT

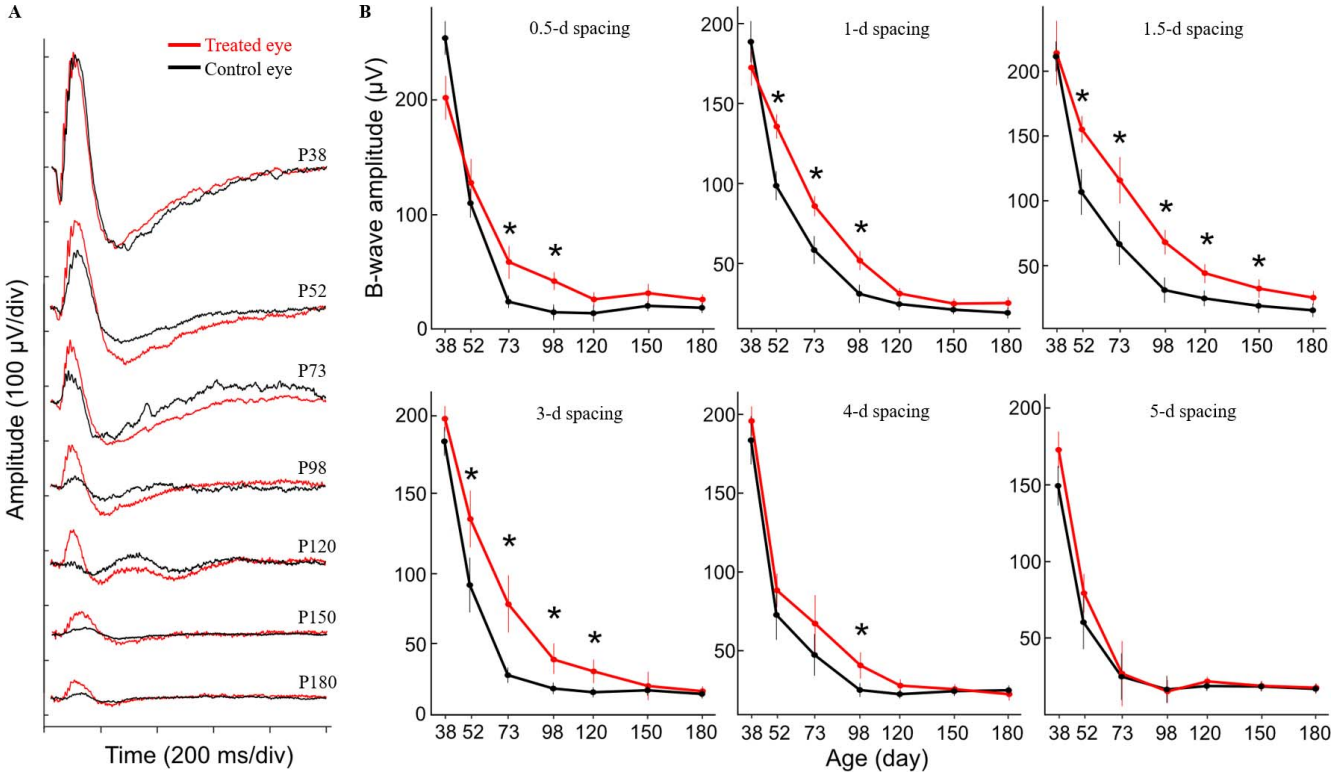


**Figure 2.** (A) Representative series of ERGs from RCS rats treated with 1.5-spot spacing laser pattern, obtained in response to flashes of 1 cd·s/m$^2$. (B). Comparison of b-wave amplitude between laser-treated and control eyes for each pattern density. Pattern density of 1.5-d spacing provides the best functional preservation. *Error bar*: SEM; *$P < 0.05$, paired *t*-test.

also demonstrated preservation of ONL only in the treated central retina, whereas little to no ONL was observed in untreated peripheral retinas, similar to the corresponding zones of control eyes (Fig. 4B).

## Retinal Histology Following Laser Photocoagulation

At P180, the histology of control eyes displayed no discernible photoreceptor layer or their nuclei (Fig. 5). Similarly, very few photoreceptor nuclei could be seen in the eyes treated with very sparse patterns: 4- and 5-d spacing. However, with denser patterns, more ONL was preserved at P180. Eyes treated with a 1.5-d spacing exhibited the best-preserved photoreceptor layer, with up to five rows of photoreceptor nuclei, and with outer segments (Fig. 5, arrow). The number of nuclei per 100 µm of length in the sections with laser patterns of various spacings and in the corresponding control eyes is summarized in the Table. The statistically significant difference between laser-treated and control eyes was noted with pattern densities of 0.5-, 1-, and 1.5-d spacing.

## Short-Term Retinal Preservation After SRT

SRT-treated eyes exhibited slight improvement in ERG compared to control eyes from P52 through P98, but it did not reach statistical significance (Figs. 6A, 6D). Serial OCT scans demonstrated thicker ONL in treated eyes, which was statistically significant at P52 and P73. However, the preservation did not last up to P180 (Fig. 6E). OCT at P52 demonstrates that ONL is preserved only in the area treated by SRT (Fig. 6B). Animals were killed for histology at P180, but no preservation benefits have been seen at that age. The number of photoreceptor nuclei per 100 µm was 3.0 ± 2.5 in the treated eyes versus 2.3 ± 1.3 in control eyes (Figs. 6C, 6F).

## No Preservation Benefits Following NRT

There were no differences in b-wave amplitudes between the eye treated with NRT and controls in the 6-month follow-up period (Figs. 7A, 7D). Similarly, no differences in ONL thickness between the treated and control eyes have been observed (Figs. 7B, 7E). Histology also demonstrated a similar number of

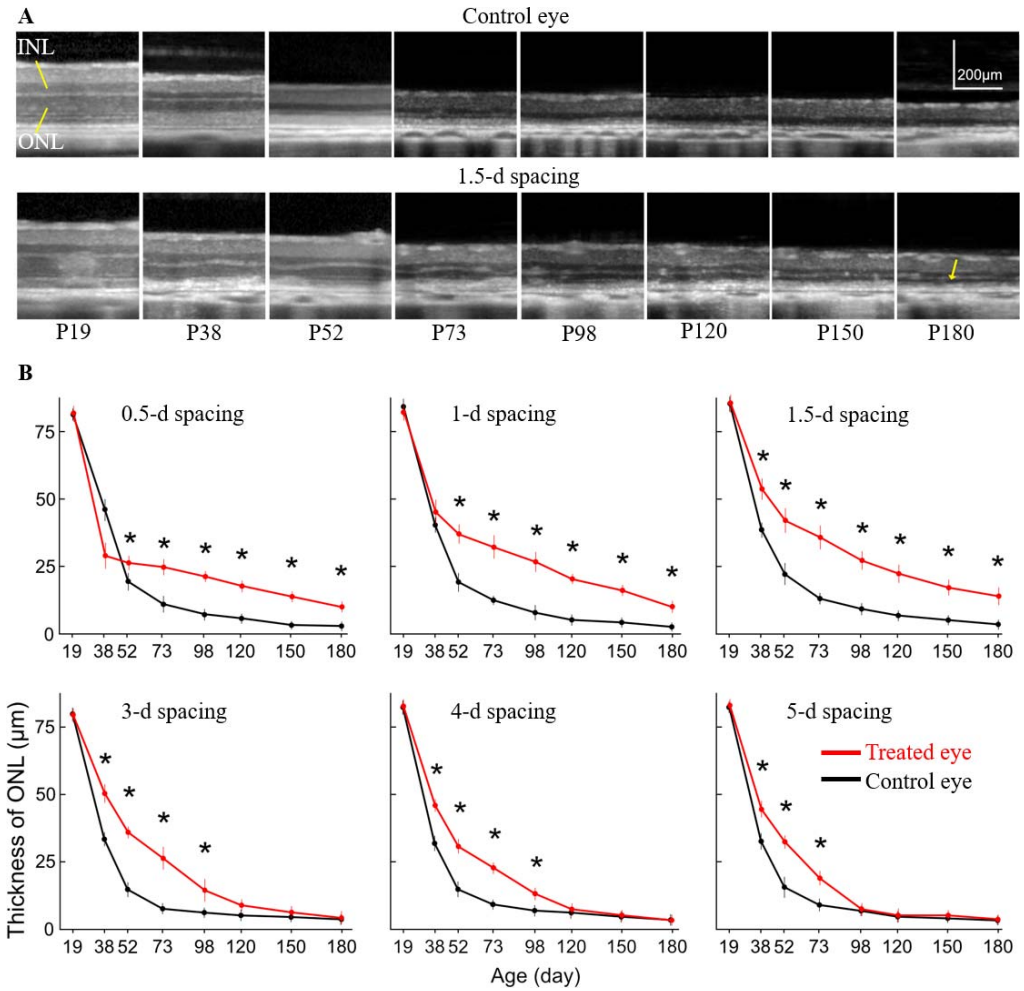


**Figure 3.** (A) Representative longitudinal OCT images from P19 to P180 illustrate the retinal degeneration in the control eye of RCS rat (*top*). Pattern laser treatment using 1.5-d spacing delays retinal degeneration and slows down the loss of ONL (*arrow*) (*bottom*). (B) ONL thickness as a function of age for each pattern density (0.5-, 1-, 1.5-, 3-, 4-, and 5-d spacing). Denser patterns (0.5-, 1.0-, 1.5-d) show better preservation of ONL compared to the control eye. In sparse patterns (3-, 4-, or 5-d), preservation of ONL was not sustained until the end of follow-up. *Error bar*: SEM; *$P < 0.05$, paired *t*-test.

nuclei in the treated and control eyes: 2.7 ± 2.0 vs. 3.3 ± 2.8, respectively (Figs. 7C, 7F).

## Discussion

Extended survival of the photoreceptors after photocoagulation in RCS rats has been noticed previously. Humphrey et al.[30] reported two to three rows of ONL remained at P83 after the following laser treatment: 300 to 350 mW, 0.5-second pulse duration, 50 μm spot diameter, 40 to 60 spots. Behbehani et al.[18] demonstrated preservation of retinal function in the laser-treated eye until P44 using the following laser parameters: 100 to 300 mW; 0.2-second pulse duration, 500-μm spot diameter, 12 spots. The present study demonstrated that the extent of retinal preservation varies with the treatment density, and under optimal conditions (40 mW, 15 milliseconds, 100 μm spots, separated by 1.5-d distance), four to five rows of photoreceptors can survive at P180, with functional benefits extending until P150. Patterns sparser than 3-d spacing did not improve the photoreceptor lifetime by much, while very dense patterns (0.5-d spacing) resulted in excessive damage with no additional benefits compared to 1.5-d spacing.

The exact mechanism leading to photoreceptors' survival after photocoagulation in RCS rats remains unknown. Several mechanisms have been suggested: enhanced phagocytosis of RPE following laser photocoagulation,[18,19] suppression of the photorecep-

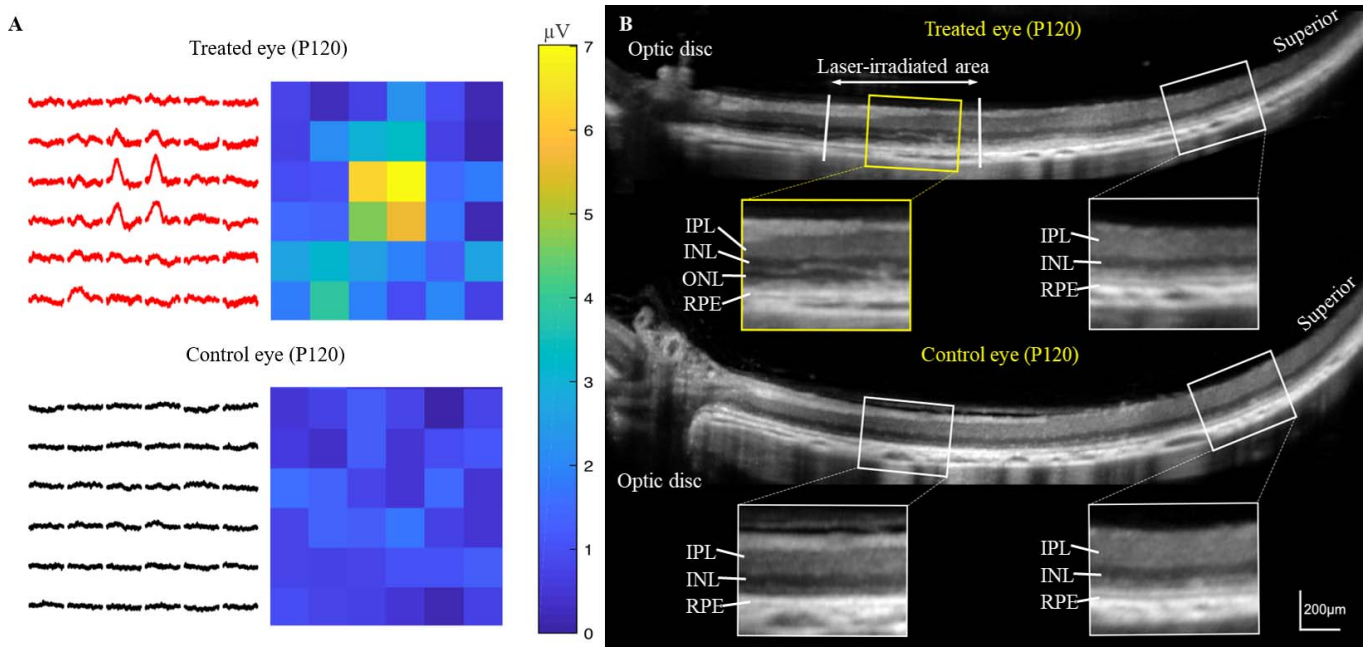


**Figure 4.** ERG and OCT in RCS rat treated with laser pattern of 1.5-d spacing, at P120. (A) Multifocal ERG responses were detected only in the laser-treated area, while in untreated retina of the same eye and in the fellow eye they were nearly flat. (B) The ONL is still present (*upper yellow box*) in the laser-treated zone, unlike the untreated retina (*upper white box*) in the same eye, and the fellow eye (*lower two white boxes*).

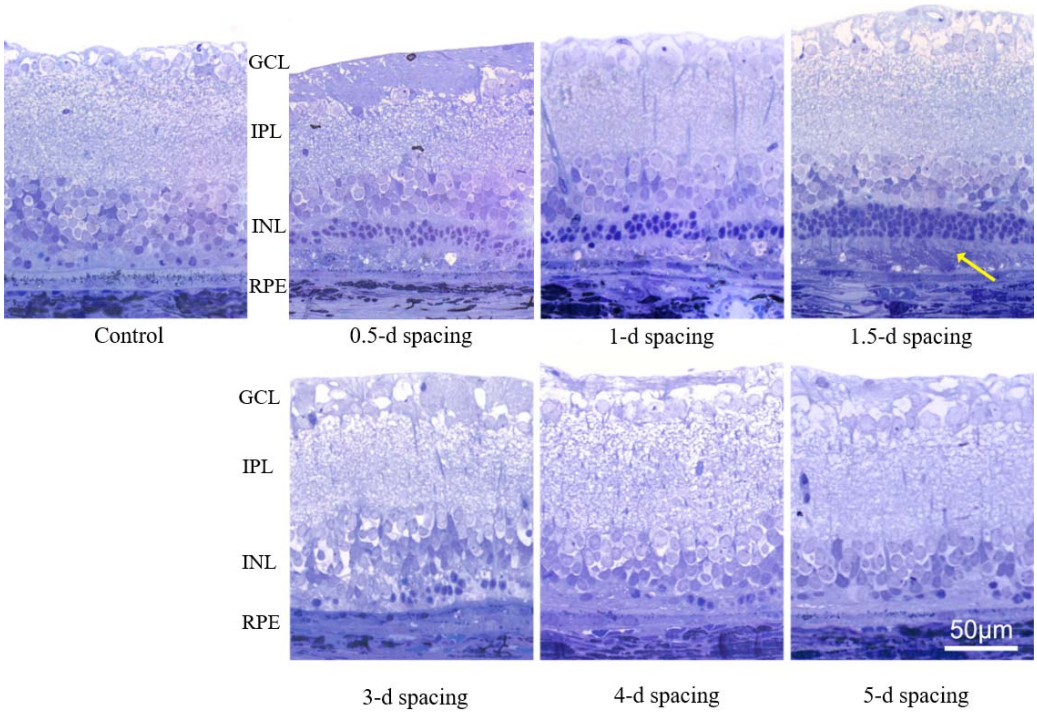


**Figure 5.** Representative histology of the retina at P180 after laser treatment with various pattern densities. Very few photoreceptor nuclei can be seen in the control eye, as well as in the retina treated with very sparse patterns: 4- and 5-d spacing. With other pattern densities, rows of photoreceptor nuclei are observed. The thickest ONL and even the inner and outer segments (*arrow*) were visible in the eyes treated with the 1.5-d patterns.

**Table.** The Number of Photoreceptor Nuclei in Laser-Treated and Control Eyes With Six Different Laser Pattern Densities

| Spacing, d | 0.5 | 1 | 1.5 | 3 | 4 | 5 |
|---|---|---|---|---|---|---|
| Treated | 17.2 ± 5.4* | 16.2 ± 5.5* | 30.8 ± 14.3* | 3.1 ± 2.3 | 2.5 ± 1.5 | 2.1 ± 1.9 |
| Control | 3.3 ± 2.8 | 2.4 ± 3.2 | 3.4 ± 3.7 | 2.9 ± 3.0 | 3.5 ± 3.0 | 1.8 ± 1.9 |

* $P < 0.05$.

tor apoptosis due to expression of neurotrophic factors such as basic fibroblast growth factor[17] or ciliary neurotrophic factor,[31] and activation of other phagocytic cells, such as microglia or macrophages, following photocoagulation.[20] Another mechanism could be the balance in supply and demand of the outer segment recycling. That is, if the load of shed outer segments is sufficiently low, even the diseased RPE cells might be able to sustain it, thus avoiding the accumulation of outer segments. Therefore, elimination of some fraction of photoreceptors by laser might decrease the daily load of shed outer segments to a sustainable level. With this in mind, the main focus of the current study was determination of the fraction of eliminated photoreceptors necessary for the best structural and functional outcomes.

If the photocoagulation zone matches the laser spot diameter, a laser pattern with 1.5-d spacing should eliminate 13% of photoreceptors within the irradiated area. It is unlikely that such a small decrease in the POS shedding would compensate for the RPE deficiency. Moreover, increasing pattern density to 0.5-d spacing, which should eliminate 35% of photoreceptors, did not improve their survival

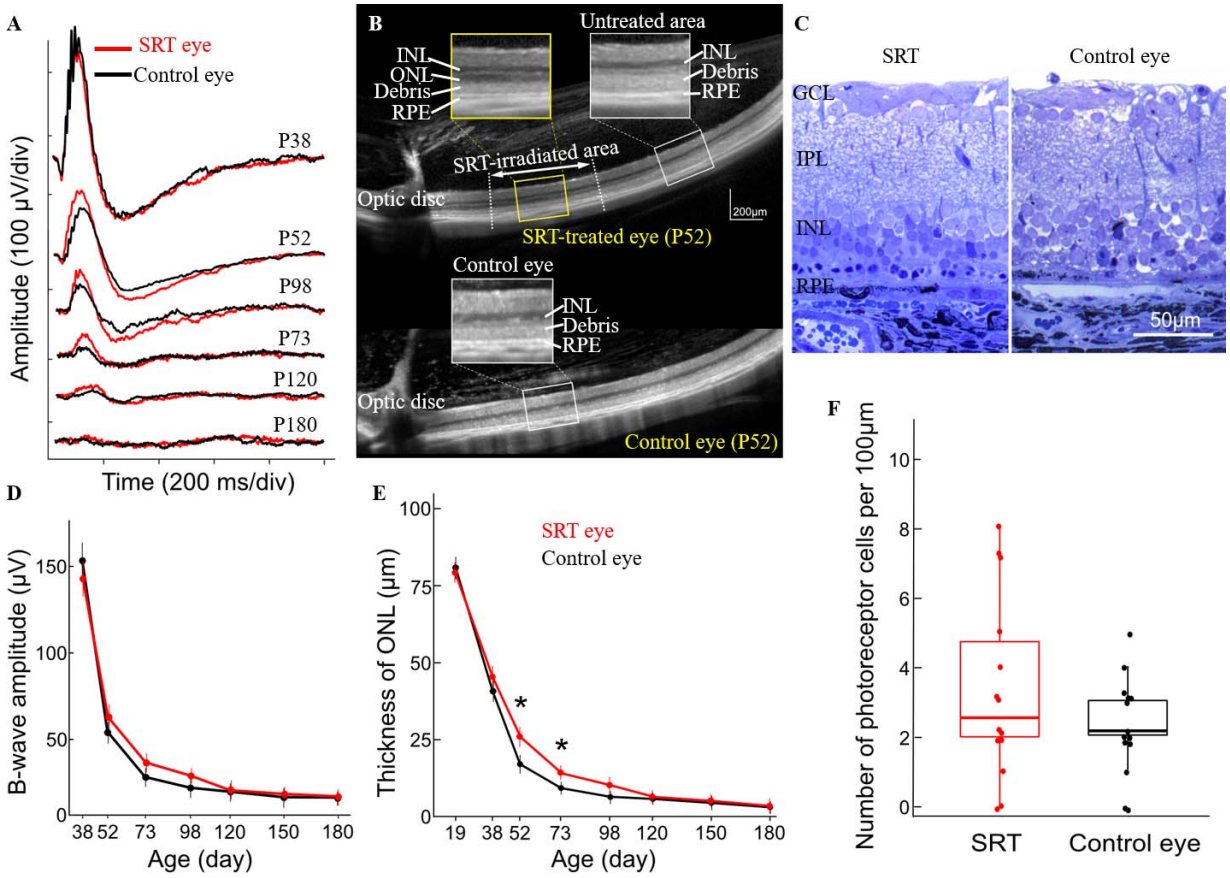


**Figure 6.** (A, D) Representative ERG waveforms from eyes treated with SRT and corresponding amplitude of the b-wave as a function of age. There is no significant difference in ERG response between the treated and control eyes. (B, E) OCT images at P52 and ONL thickness plotted as a function of age. Significant preservation of ONL was observed only at P52 and P73. (C, F) Histology at P180 and the average number of photoreceptor nuclei per 100 µm demonstrated no significant difference between the SRT-treated and control eyes.

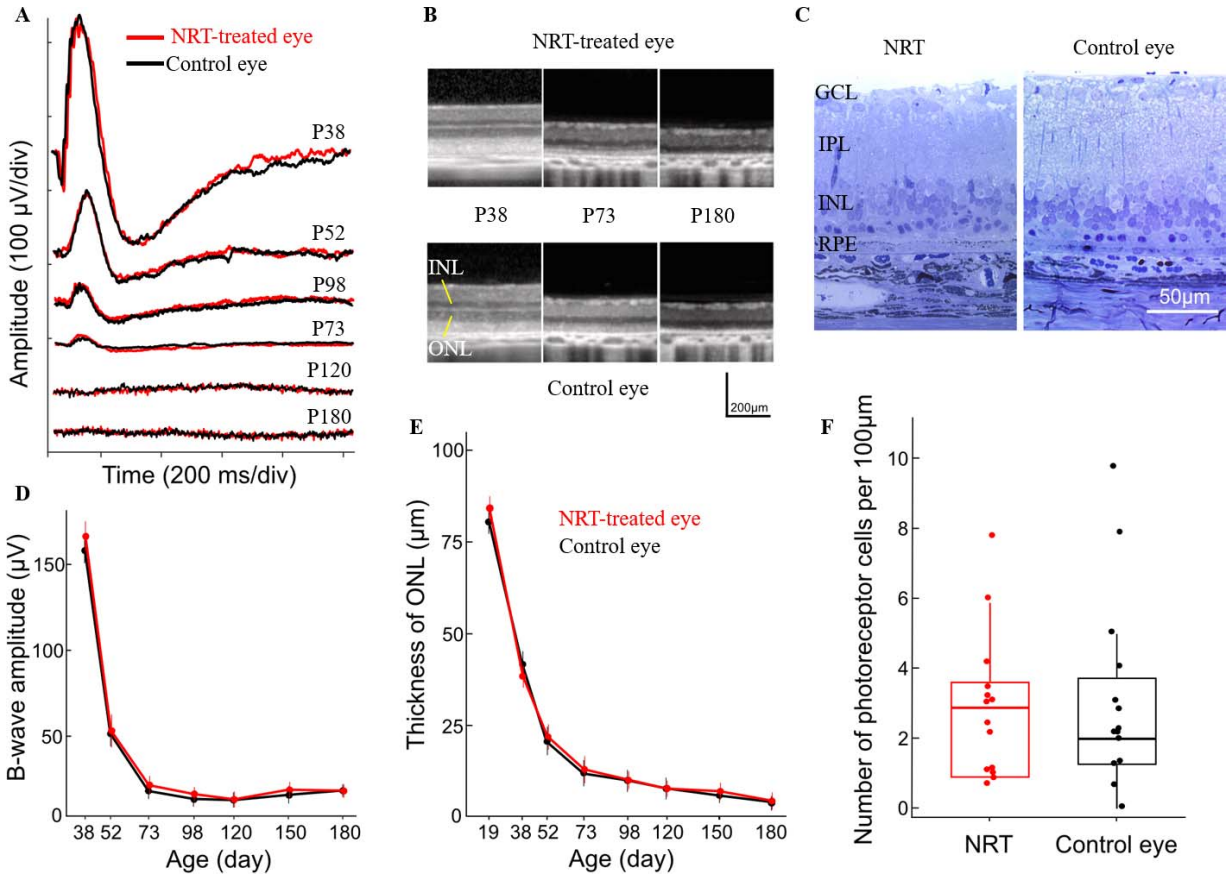


**Figure 7.** (A, D) Representative ERG waveforms from the eyes treated with NRT and the corresponding b-wave amplitude as a function of age. Electophysiologically, there is no significant difference between the treated and control eyes. (B, E) Serial OCT images from the treated and control eyes and ONL thickness as a function of age. No preservation of ONL was not observed. (C, F) Retinal histology from the treated and control eyes at P180 and the number of the photoreceptor nuclei per 100 μm are also very similar.

either. These observations indicate that the hypothesis of the supply–demand balance in POS recycling is unlikely to be correct.

However, even a temporary rescue of photoreceptors could provide very significant clinical benefit. At optimal settings (1.5-d spacing) photoreceptor survival, as judged by the ONL thickness on OCT images, was extended from 73 to 180 days—by a factor of 2.5. If similar extension could be achieved in human patients, it would extend the lifetime of vision from teenage to mid-30s, a very significant improvement, especially considering the simplicity of the treatment.

One limitation is that laser photocoagulation can't be applied directly to the central fovea, which is responsible for the central vision. Therefore, nondestructive and noninvasive laser treatment, such as SRT or NRT, are very appealing potential alternatives, if they would be effective. Selective destruction of RPE using microsecond pulses[25,26] without thermal damage to photoreceptors in SRT has been successfully tested in clinics to treat various retinal diseases. Its therapeutic effect is thought to be based on replacement of the old RPE cells with newly proliferated ones, hence rejuvenating the RPE layer. However, the current study demonstrated that a single application of SRT at P19, just before the accumulation of subretinal debris, provided morphologic preservation of photoreceptors for a short period (from P52 to P73) in the treated area. It well may be that repeating SRT could extend the photoreceptor preservation further, but we could not do it because the subretinal debris accumulating after P19 scattered the laser light and interfered with photocoagulation, which we used for titration of laser power. Recently developed real-time dosimetry systems based on optoacoustics[32] and reflectometry[33] may permit laser titration even with the debris present. This would allow determination of whether SRT retreatments could extend the rescue of photoreceptors further.

Recently, efficacy of NRT has been shown in treatment of various retinal disorders, including central serous chorioretinopathy and macular telangiectasia.[24] The effect of nondamaging hyperthermia has mainly been attributed to upregulation of the heat-shock proteins, leading to stimulation of not only the RPE, but also Muller cells[24] and microglia.[34] In particular, sublethal laser exposure potentiates microglial cell phagocytic activity,[34] which could be useful to clear the accumulated outer segments of photoreceptors. However, in the current study NRT did not show any benefits for morphologic or functional preservation of photoreceptors in RCS rats. This result indicates that simply boosting the metabolism of RPE cells is not sufficient for photoreceptor preservation, and physical removal of a fraction of photoreceptors is essential for prolonging their survival.

In conclusion, destruction of about 15% of the photoreceptors promotes survival of the remaining photoreceptors in the MERTK-related RP. This approach can be easily tested in human patients by pattern photocoagulation in a periphery before it completely degenerates. Loss of one-seventh of photoreceptors by small-spot coagulation and without scarring should not diminish retinal sensitivity, as has been shown in this study, while it may significantly extend the lifetime of the visual function.

## Acknowledgments

Supported by a Stanford Photonics Research Center Grant.

Disclosure: **S. Kang**, None; **H. Lorach**, None; **M.B. Bhuckory**, None; **Y. Quan**, None; **R. Dalal**, None; **D. Palanker**, None

## References

1. Hamel C. Retinitis pigmentosa. *Orphanet J Rare Dis*. 2006;1:40.
2. Hartong DT, Berson EL, Dryja TP. Retinitis pigmentosa. *Lancet*. 2006;368:1795–1809.
3. Ghazi NG, Abboud EB, Nowilaty SR, et al. Treatment of retinitis pigmentosa due to MERTK mutations by ocular subretinal injection of adeno-associated virus gene vector: results of a phase I trial. *Hum Genet*. 2016;135:327–343.
4. Bainbridge JWB, Smith AJ, Barker SS, et al. Effect of gene therapy on visual function in Leber's congenital amaurosis. *N Engl J Med*. 2008;358:2231–2239.
5. Siqueira RC, Messias A, Voltarelli JC, et al. Intravitreal injection of autologous bone marrow-derived mononuclear cells for hereditary retinal dystrophy: a phase I trial. *Retina*. 2011;31:1207–1214.
6. Park SS, Bauer G, Abedi M, et al. Intravitreal autologous bone marrow CD34+ cell therapy for ischemic and degenerative retinal disorders: preliminary phase 1 clinical trial findings. *Invest Ophthalmol Vis Sci*. 2014;56:81–89.
7. Sieving PA, Caruso RC, Tao W, et al. Ciliary neurotrophic factor (CNTF) for human retinal degeneration: Phase I trial of CNTF delivered by encapsulated cell intraocular implants. *Proc Natl Acad Sci U S A*. 2006;103:3896–3901.
8. Farvardin M, Afarid M, Attarzadeh A, et al. The Argus-II retinal prosthesis implantation; from the global to local successful experience. *Front Neurosci*. 2018;12:584.
9. Daiger SP, Sullivan LS, Bowne SJ. Genes and mutations causing retinitis pigmentosa. *Clin Genet*. 2013;84:132–141.
10. Oishi M, Oishi A, Gotoh N, et al. Comprehensive molecular diagnosis of a large cohort of Japanese retinitis pigmentosa and usher syndrome patients by next-generation sequencing. *Invest Ophthalmol Vis Sci*. 2014;55:7369–7369.
11. Evans DR, Green JS, Johnson GJ, et al. Novel 25 kb deletion of MERTK causes retinitis pigmentosa with severe progression. *Invest Ophthalmol Vis Sci*. 2017;58:1736–1737.
12. Gal A, Li Y, Thompson DA, et al. Mutations in MERTK, the human orthologue of the RCS rat retinal dystrophy gene, cause retinitis pigmentosa. *Nat Genet*. 2000;26:270–271.
13. Nandrot EF, Dufour EM. Mertk in daily retinal phagocytosis: a history in the making. In: *Retinal Degenerative Diseases*. Vol 664. Advances in Experimental Medicine and Biology. New York, NY: Springer; 2010:133–140.
14. Deng WT, Dinculescu A, Li Q, et al. Tyrosine-mutant AAV8 delivery of human MERTK provides long-term retinal preservation in RCS rats. *Invest Ophthalmol Vis Sci*. 2012;53:1895–1904.
15. Smith AJ, Schlichtenbrede FC, Tschernutter M, et al. AAV-mediated gene transfer slows photoreceptor loss in the RCS rat model of retinitis pigmentosa. *Mol Ther*. 2003;8:188–195.

16. LaVail MM, Yasumura D, Matthes MT, et al. Gene therapy for MERTK-associated retinal degenerations. *Adv Exp Med Biol*. 2016;854:487–493.
17. Xiao M, Sastry SM, Li ZY, et al. Effects of retinal laser photocoagulation on photoreceptor basic fibroblast growth factor and survival. *Invest Ophthalmol Vis Sci*. 1998;39:618–630.
18. Behbehani MM, Bowyer DW, Ruffolo JJ, Kranias G. Preservation of retinal function in the RCS rat by laser treatment. *Retina*. 1984;4:257–263.
19. Ansell PL, Marshall J. Laser induced phagocytosis in the pigment epithelium of the Hunter dystrophic rat. *Br J Ophthalmol*. 1976;60:819–828.
20. Lorach H, Kang S, Dalal R, et al. Long-term rescue of photoreceptors in a rodent model of retinitis pigmentosa associated with MERTK mutation. *Sci Rep*. 2018;8:11312.
21. Kang S, Park Y-G, Kim JR, et al. Selective retina therapy in patients with chronic central serous chorioretinopathy: a pilot study. *Medicine (Baltimore)*. 2016;95:e2524.
22. Park Y-G, Kim JR, Kang S, et al. Safety and efficacy of selective retina therapy (SRT) for the treatment of diabetic macular edema in Korean patients. *Graefes Arch Clin Exp Ophthalmol*. 2016;254:1703–1713.
23. Roider J. Selective retina therapy (SRT) for clinically significant diabetic macular edema. *Graefes Arch Clin Exp Ophthalmol*. 2010;248:1263–1272.
24. Lavinsky D, Wang J, Huie P, et al. Nondamaging retinal laser therapy: rationale and applications to the macula. *Invest Ophthalmol Vis Sci*. 2016;57:2488–2500.
25. Roider J, Michaud NA, Flotte TJ. Response of the retinal pigment epithelium to selective photocoagulation. *Arch Ophthalmol*. 1992;110:1786–1792.
26. Paulus YM, Jain A, Nomoto H, et al. Selective retinal therapy with microsecond exposures using a continuous line scanning laser. *Retina*. 2011;31:380–388.
27. Lavinsky D, Chalberg TW, Mandel Y, et al. Modulation of transgene expression in retinal gene therapy by selective laser treatment. *Invest Ophthalmol Vis Sci*. 2013;54:1873–1878.
28. Palanker D. Evolution of concepts and technologies in ophthalmic laser therapy. *Annu Rev Vis Sci*. 2016;2:295–319.
29. Sramek C, Mackanos M, Spitler R, et al. Nondamaging retinal phototherapy: dynamic range of heat shock protein expression. *Invest Ophthalmol Vis Sci*. 2011;52:1780–1787.
30. Humphrey MF, Parker C, Chu Y, Constable IJ. Transient preservation of photoreceptors on the flanks of argon laser lesions in the RCS rat. *Curr Eye Res*. 1993;12:367–372.
31. Wen R, Song Y, Cheng T, et al. Injury-induced upregulation of bFGF and CNTF mRNAS in the rat retina. *J Neurosci*. 1995;15:7377–7385.
32. Schuele G, Elsner H, Framme C, Roider J, Birngruber R, Brinkmann R. Optoacoustic real-time dosimetry for selective retina treatment. *J Biomed Opt*. 2005;10:064022.
33. Park Y-G, Seifert E, Roh YJ, et al. Tissue response of selective retina therapy by means of a feedback controlled energy ramping mode. *Clin Experiment Ophthalmol*. 2014;42:846–855.
34. Song S, Zhou F, Chen WR. Low-level laser therapy regulates microglial function through Src-mediated signaling pathways: implications for neurodegenerative diseases. *J Neuroinflammation*. 2012;9:219.